BMC Veterinary Research

RESEARCH

Open Access

Blood mir-331-3p is a potential diagnostic marker for giant panda (*Ailuropoda melanoleuca*) testicular tumor

Yan Zhu[1], Zhi Huang[1], Caiwu Li[1], Chengyao Li[1], Ming Wei[1], Linhua Deng[1], Wenwen Deng[1], Xiao Zhou[1], Kai Wu[1], Bo Yang[1], Yuanyuan Qu[1], Qin Liu[1], Xuemei Chen[1], Desheng Li[1*] and Chengdong Wang[1*]

Abstract

Background In recent years, several giant pandas have suffered from testicular tumor, which has seriously affected giant panda health. However, the pathogenesis of testicular tumor in giant panda is still unclear. Studies have shown that miRNAs are involved in the occurrence and development of a variety of cancers. However, the effect of miRNAs on giant panda testicular tumor has been little studied. Therefore, this study explored the pathogenesis of giant panda testicular tumor through miRNA and mRNA sequencing, and screened out diagnostic markers of testicular tumor.

Results Combined with phenotypic symptoms and pathological section results, three giant pandas were diagnosed with testicular tumor and divided into tumor group, and three other giant pandas were divided into normal group. A total of 29 differentially expressed miRNAs (DEmiRNAs) were screened by blood miRNA-seq, and 3149 target gene candidates were predicted. Functional enrichment analysis showed that the target genes were mainly involved in intermembrane lipid transfer and ATP-dependent chromatin remodeling. However, only 5 DEmiRNAs were screened by miRNA-seq of blood-derived exosomes and 364 target genes were predicted, which were mainly involved in antigen processing and presentation. In addition, 216 differentially expressed genes (DEGs) were screened by RNA-seq, and functional enrichment analysis showed that tumor-specific DEGs significantly enriched to protein phosphorylation. Spearman correlation analysis of miRNA-mRNA showed that the expressions of miR-331-3p and *PKIG* were significantly positively correlated (spearman = 0.943, $p < 0.01$), while the expressions of miR-331-3p and *ENSAMEG00000013628* were significantly negatively correlated (spearman= -0.829, $p < 0.05$). RT-PCR showed that the expression of miR-331-3p was significantly decreased in giant panda with tumor ($p < 0.01$).

Conclusions blood miRNAs and exosomal miRNAs exhibit distinct regulatory patterns concerning giant panda testicular tumor, potentially reflecting divergent biological processes in the disease's etiology. Meanwhile, miR-331-3p could be used as a potential diagnostic marker for giant panda testicular tumor. Our findings are conducive to the

*Correspondence:
Desheng Li
lidesheng_ccrcgp@163.com
Chengdong Wang
Wangchengdong@aliyun.com

Full list of author information is available at the end of the article

rapid clinical diagnosis of testicular tumor in giant pandas, and are also expected to provide scientific reference for further research on the pathogenesis of testicular tumor.

Keywords miRNA sequencing, mRNA sequencing, Giant panda, Testicular tumor, Exosome, miR-331-3p

Background

In humans, testicular tumors can be classified as germ cell tumors, non-germ cell tumors, and secondary testicular tumors. 95% of testicular tumors are testicular germ cell tumors, which are mainly divided into two categories: seminoma and non-seminoma [1, 2]. Seminoma is the most common testicular tumor, accounting for about 50% of germ cell tumors and 40–45% of testicular tumors [3]. Testicular tumor is a zoonotic disease that occurs in cats, dogs, pigs, cattle, horses, rabbits, chickens, and other animals, among which dogs have the highest incidence and occur at any age, especially in old dogs [4]. However, in recent years, we have found that giant pandas also suffer from testicular tumor. In 2014, a giant panda named Gaogao showed swelling symptoms on the left testicle, the testicular parenchymal structure was basically lost, and he was eventually diagnosed with testicular tumor. Subsequently, giant pandas named Ximeng, Yaxiang, and Yunzi were diagnosed with testicular tumor. China Conservation and Research Center for the Giant Panda (CCRCGP) has the world's largest captive giant panda population, up to now, we have found about 8 cases of testicular tumors in giant pandas. Although the clinical data are few, it is necessary to conduct research on testicular tumors in order to better protect the health of giant pandas. However, testicular tumor in giant pandas has not been explored in depth, so their pathogenesis is almost unknown.

Studies have shown that one of the main communication pathways between tumor cells and their environment is exosomes [5], a novel class of substances that mediate intercellular signaling and contain a variety of biomolecules, such as lipids, proteins, and nucleic acids. miRNAs are important exosomal components, and they are a class of short ncRNAs that are most widely studied at present. miRNAs regulate the expression of target genes at the post-transcriptional level and are involved in a variety of cellular processes, including cell proliferation, differentiation, and apoptosis [6]. Exosomal miRNAs are involved in the occurrence and development of various cancers [7]. Studies have confirmed that exosomal miRNAs are closely related to the occurrence, development, clinical classification and early diagnosis of hepatocellular carcinoma [8], pancreatic cancer [9], breast cancer [10], ovarian cancer [11], and prostate cancer [12, 13]. For example, in prostate cancer patients, exosomal miR-182 and miR-183 are highly expressed [12], and miR-375 and miR-1290 in exosomes can be used to evaluate the prognosis of prostate cancer patients [13]. Therefore, exosomal miRNA is considered as a promising tumor biomarker. However, the regulatory role of exosomal miRNA in giant panda testis tumor has not been studied.

In this study, Gaogao, Ximeng, and Yaxiang were divided into tumor group, and Daili, Linyang and Tongtong were divided into normal group. Firstly, compared with normal group, we screened DEmiRNAs from tumor blood by miRNA-seq. Subsequently, exosomes were isolated from plasma and DEmiRNAs in exosomes were analyzed. Combined with functional enrichment analysis, the regulatory patterns of the blood DEmiRNAs and exosomal DEmiRNAs were predicted respectively. Besides, we also screened the DEGs from blood by mRNA-seq and performed functional enrichment analysis, and finally, the diagnostic marker of giant panda testicular tumor was verified by spearman correlation analysis and qRT-PCR. Our findings indicated that blood miRNAs and exosomal miRNAs exhibit distinct regulatory patterns concerning giant panda testicular tumor, potentially reflecting divergent biological processes in the disease's etiology. Meanwhile, miR-331-3p could be used as a potential diagnostic marker for giant panda testicular tumor. These insights are conducive to the rapid clinical diagnosis of testicular tumor in giant pandas, and are anticipated to offer a scientific basis for future investigations into the underlying causes of giant panda testicular tumor.

Methods

Sample collection

All giant pandas used in this research were sourced from Dujiangyan Base in China Conservation and Research Center for the Giant Panda, and they were in normal conscious state when their blood was collected. The whole blood samples of 6 giant pandas (Table 1) were collected with EDTA anticoagulant collection vessels and mixed upside down, and no less than 10mL of blood was collected from each giant panda. At 4 ℃, the horizontal rotor was centrifuged at 1900xg for 10 min, and the upper plasma was absorbed into a new centrifuge tube, centrifuged at 4℃ and 3000xg for 15 min. The plasma was carefully sucked out and packaged, and stored at -80℃ for later use.

Exosome extraction

Exosomes were extracted by ultracentrifugation. At 4℃, plasma samples were centrifuged at 2000xg for 30 min. The supernatant was carefully transferred to a new centrifuge tube at 4℃, 10,000xg, for 45 min to remove large

Table 1 Basic information of experimental giant pandas

Name	Stud#	Sex	Birth date	Location	Condition
Ximeng	399	Male	1993.9.19	Dujiangyan Base, China	Testicular tumor
Yaxiang	529	Male	2001.8.20	Dujiangyan Base, China	Testicular tumor
Gaogao	415	Male	1990.9.1	Dujiangyan Base, China	Testicular tumor
Daili	542	Male	1999.9.1	Dujiangyan Base, China	Healthy
Linyang	538	Male	2001.9.28	Dujiangyan Base, China	Healthy
Tongtong	586	Male	2004.8.30	Dujiangyan Base, China	Healthy

vesicles. Take the supernatant and filter it with 0.45 μm filter membrane (Millipore, R6BA09493). The filtrate was centrifuged at 4℃, 100,000xg, for 70 min. After the supernatant was abandoned and the precipitation was re-suspended with 10 mL precooled 1×PBS, the exosomes were obtained by centrifugation at 4℃, 100,000xg, for 70 min. Finally, the exosomes were suspended with 300μL pre-cooled PBS, 20μL was prepared for transmission electron microscopy (TEM) (Hitachi, HT-7700), 10μL for particle size detection, 60μL for Western blot, and the remaining exosomes were stored at -80℃.

TEM and particle size detection

10μL exosome drops were added to the copper mesh and placed for 1 min. The float was absorbed with filter paper. Add 10μL uranyl acetate to copper mesh, stain for 1 min, and then blot the float with filter paper. After drying at room temperature for 10 min, the exosomes were examined by TEM at 100 kV to identify the physical characteristics of the exosomes. In the particle size detection, the performance of the particle size analyzer (NanoFCM, N30E) should be tested with standard products first, and the exosome sample can be loaded only after the test is passed. The exosomes were diluted from 10μL to 30μL with PBS and mixed evenly with a vortex mixer. The samples were slowly injected into the sample pool with a syringe to determine the size and concentration of exosomes.

Western blot (WB)

The protein concentration of exosomes was determined by BCA method. After the protein was denatured by boiling, the samples were taken by electrophoresis using 10% SDS-PAGE protein separation glue with 10 μg per hole. After the protein separation, the membrane was transferred to PVDF membrane with a constant current of 300 mA for 80 min and closed with TBST containing 5% skim milk for 1 h. CD9 primary antibody was incubated overnight at 4℃ (Abclonal, 1:1000). After cleaning, the Goat anti-Rabbit second antibody (Merck Millipore, 1:5000) was incubated with the second antibody for 1 h. The mixture of ECLA/B was added and incubated for 5 min in dark light, and the image was taken by chemiluminescent gel imaging system (CLINX, ChemiScope 3000mini).

Small RNA sequencing and bioinformation analysis

Total RNA from giant panda blood and blood-derived exosomes was extracted, and small RNA library was constructed using Small RNA Sample Pre Kit (Illumina). Using total RNA as the starting sample, small RNA is directly combined with splicing on both ends, then cDNA is synthesized by reverse transcription, and then PCR amplification and PAGE electrophoresis are used to obtain cDNA libraries with 18–35 nucleotide (nt) insertions. Finally, sequencing was performed on the Illumina SE50 platform (Novo, Beijing). After the quality control of the raw sequencing data, the clean reads were classified and annotated. To make every unique small RNA mapped to only one annotation, we followed the priority rule: known miRNA> rRNA > tRNA > snRNA > snoRNA > repeat > gene > NAT-siRNA > gene > novel miRNA > ta-siRNA. The total rRNA proportion was used as a marker for sample quality indicator and it should be less than 40% in animal samples as high quality. The expression level of miRNA was estimated by TPM (transcript per million) through the following criteria: normalized expression = mapped readcount/total reads*1,000,000 [14]. As our samples have three biological replicates, differential expression analysis of each comparison group was performed using the R package DESeq2 [15]. The p-values were adjusted using the Benjamini & Hochberg method and corrected p-value of 0.05 was set as the threshold for significant differential expression by default [16]. The target gene candidates were predicted by miRanda and RNAhybrid software [17, 18]. Gene ontology (GO) and Kyoto Encyclopedia of Genes and Genomes (KEGG) pathway enriched in target gene candidates of DEmiRNAs were deciphered using the GOseqR package [19] and KOBAS [20] software, respectively.

RNA sequencing and bioinformation analysis

Total RNA from giant panda blood was extracted, and RNA library was constructed using RNA Library Prep Kit for Illumina® (NEB, USA). Briefly, mRNA with poly-A tail was enriched by Oligo (dT) magnetic beads, and then the mRNA was randomly interrupted by divalent cations in Fragmentation Buffer. The purified double-stranded cDNA was end-repaired, A tail was added and a sequencing connector was connected. cDNA about 370–420 bp was screened by AMPure XP beads for

PCR amplification, and PCR products were purified by AMPure XP beads again. Finally, the library is obtained. RNA sequencing was performed on the Illumina SE50 platform (Novo, Beijing) after the library was qualified. After the quality control of the raw sequencing data, the clean reads and reference genomes were compared using the HISAT2 software. Here are reference genome FA information (https://ftp.ensembl.org/pub/release-110/fasta/ailuropoda_melanoleuca/dna/) and annotation file GTF information (https://ftp.ensembl.org/pub/release-110/gtf/ailuropoda_melanoleuca/). The expression level of mRNA was estimated by FPKM (Fragments Per Kilobase of exon model per Million mapped fragments). As our samples have three biological replicates, differential expression analysis of each comparison group was performed using the R package DESeq2 [15]. The p-values were adjusted using the Benjamini & Hochberg method and corrected p-value of 0.05 was set as the threshold for significant differential expression by default [16]. GO and KEGG enrichment analysis of DEGs was performed by clusterProfiler software [21].

Correlation analysis and RT-PCR validation

R version 4.4.0 was used to analyze the spearman correlation between the DEGs obtained by RNA sequencing and the target genes of the DE miRNAs obtained by sRNA sequencing (p-value < 0.05). Then, mRNA and miRNA from Total RNA were reverse-transcribe into cDNA using PrimeScript RT reagent Kit with gDNA Eraser and Mir-X™ miRNA First Strand Synthesis Ki, respectively. Finally, we used the SYBR Premix Ex Taq II (TaRaKa, China) for RT-PCR. *GAPDH* and *U6* were used as endogenous controls. Three technical replicates were set for each response, and quantitative data were analyzed by $2^{-\triangle\triangle Ct}$.

Table 2 List of abbreviations

Abbreviation	Name
miRNA	microRNA
DEmiRNAs	Differentially expressed miRNAs
DEGs	Differentially expressed genes
RNA-seq	RNA-sequencing
PCR	Polymerase chain reaction
WB	Western blot
EDTA	Ethylenediamine tetraacetic acid
PBS	Phosphate buffered saline
TEM	Transmission electron microscopy
TPM	Transcript per million
FPKM	Fragments per kilobase of exon model per million mapped fragments
GO	Gene ontology
KEGG	Kyoto encyclopedia of genes and genomes
PKIG	protein kinase inhibitor gamma

Statistical analysis

Excel 2019, GraphPad Prism 7.0 and AI software were used for data analysis and mapping respectively. Data were shown as the mean ± S.D., and values of $p < 0.05$ were considered statistically significant (* $p < 0.05$, ** $p < 0.01$).

List of abbreviations

Abbreviations are shown in Table 2.

Results

Testicular tumor of giant panda

In recent years, there have been several cases of giant pandas suffering from testicular tumor in China Conservation and Research Center for the Giant Panda (CCRCGP). Since 2014, Gaogao, Ximeng, and Yaxiang were diagnosed with testicular tumor. Phenotypic characteristics showed that the size of diseased testis was twice that of normal testis, and diseased testis became harder (Fig. 1A). Pathological section showed that normal testis had clear seminiferous tubules and intact testicular tissue structure (Fig. 1B), while diseased testis showed the testicular parenchymal structure was basically lost, and no intact and clear seminiferous tubules were observed, which have been replaced by elliptical or oblate parenchymal cells (Fig. 1C) (Additional file S1).

Differential expression and functional enrichment of blood miRNAs in giant panda testicular tumor

Small RNA libraries of giant panda blood were established for high-throughput sequencing. The length distribution of small RNA was mainly 18-26nt, and concentrated in 21-23nt (Fig. 2A). Clean reads in all samples were annotated as known miRNA (53.88%), rRNA (0.01%), tRNA (0.04%), snRNA (0.01%), snoRNA (0.03%), repeat (0.28%), exon (0.15%), intron (0.32%) and others (45.28%) (Fig. 2B). A total of 400 miRNAs were identified from the six giant pandas's blood. TPM density showed the miRNA expression levels were consistent in each giant panda (Fig. 2C). In addition, compared to normal group, we found a total of 29 DEmiRNAs in tumor group, of which 26 were up-regulated and 3 were down-regulated (Fig. 2D). The hierarchical cluster analysis of DEmiRNAs showed tumor-specific miRNAs expressed patterns, and the three biological repetitions of normal group were well assembled into one cluster. However, Gaogao did not cluster well in the tumor samples (Fig. 2E), and we speculated that there may be individual differences.

Next, RNAhybrid and miRanda software were used to predict the target gene candidates of all DEmiRNAs, and a total of 3149 target gene candidates were predicted. GO and KEGG enrichment analyses were performed using the predicted target gene candidates. Based on the

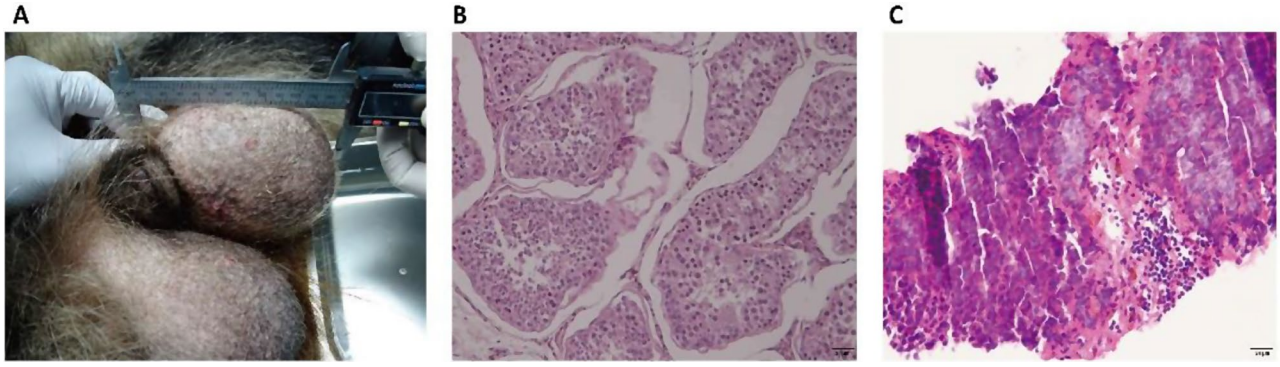

Fig. 1 Testicular tumor of giant panda. **A** Measurement of the testicular tumors. **B** Photomicrographs of HE stained normal testis. Scale bar, 20 μm. **C** Photomicrographs of HE stained testicular tumors. Scale bar, 20 μm

standard with corrected p-value < 0.05, we found that the target gene candidates were mainly involved in biological processes such as intermembrane lipid transfer and negative regulation of binding, while molecular function and cellular components were almost not involved (Fig. 2F). KEGG analysis showed the relevant signaling pathways were mainly concentrated in hypertrophic cardiomyopathy, ATP-dependent chromatin remodeling, and protein digestion and absorption (Fig. 2G).

Isolation and identification of exosomes derived from giant panda blood

Exosomes are extracellular vesicles that are rich in biological information. In this study, exosomes were extracted by ultracentrifugation method, and the extracted exosomes were identified by TEM, particle size detection and Western blot. We observed the extracted exosomes showed round or cup-shaped vesicles through TEM (Fig. 3A). Its diameter was measured between 30 and 150 nm (Fig. 3B), which is consistent with the diameter distribution of normal exosomes. In addition, Western blot analysis was performed with the exosome-specific antibody CD9, and the results showed that CD9 was positive in the giant panda exosome samples (Fig. 3C) (Additional file S2). The above results indicate we have successfully extracted exosomes from giant panda blood.

Differential expression and functional enrichment of exosomal miRNAs in giant panda testicular tumor

We extracted RNA from exosomes and established the small RNA library of giant panda blood exosomes. The length distribution of small RNA was mainly 18-35nt, and they were concentrated in 22nt and 23nt, showing a bimodal distribution (Fig. 4A), which was consistent with previous studies [22]. Clean reads obtained after quality control were annotated as known miRNA (7.95%), rRNA (0.01%), tRNA (0.01%), snRNA (0.00%), snoRNA (0.01%), repeat (1.13%), exon (0.01%), intron (0.04%) and others (90.83%) (Fig. 4B). A total of 382 miRNAs were identified from exosomes. TPM density showed that the miRNA expression levels were consistent in the exosome of each giant panda (Fig. 4C). However, we found there were only 5 DEmiRNAs, of which 2 were up-regulated (miR-574-5p, miR-200a-3p) and 3 were down-regulated (miR-222-3p, miR-3074-5p, miR-24-3p) (Fig. 4D). The hierarchical cluster analysis of DEmiRNAs showed tumor-specific miRNAs expressed patterns, and the three biological repetitions of each group were well assembled into one cluster (Fig. 4E). Therefore, we speculated that exosomal miRNAs may have different regulatory patterns compared with blood miRNAs.

Then, a total of 364 target gene candidates were predicted for DEmiRNAs, and functional enrichment analysis showed that these target gene candidates were mainly involved in cellular components such as molybdopterin synthase complex, and molecular biological function such as organic acid: sodium symporter activity and sodium: dicarboxylate symporter activity (Fig. 4F). KEGG analysis showed that the signaling pathway was mainly focused on antigen processing and presentation (Fig. 4G).

Differential expression and functional enrichment of blood mRNAs in giant panda testicular tumor

Expression patterns of blood mRNAs in giant panda testicular tumor was identified by RNA-seq. The results of FPKM density showed that mRNA expression levels of each giant panda were almost consistent (Fig. 5A). In addition, compared to normal group, a total of 216 DEGs were found in tumor group, of which 136 were up-regulated and 80 were down-regulated (Fig. 5B). The hierarchical cluster analysis of DEGs showed tumor-specific gene expressed patterns, and the three biological repetitions of each group were well assembled into one cluster (Fig. 5C).

Then, the GO enrichment and KEGG enrichment analyses were performed separately. Overall, with corrected p-value<0.05, tumor-specific DEGs significantly enriched to dephosphorylation and protein

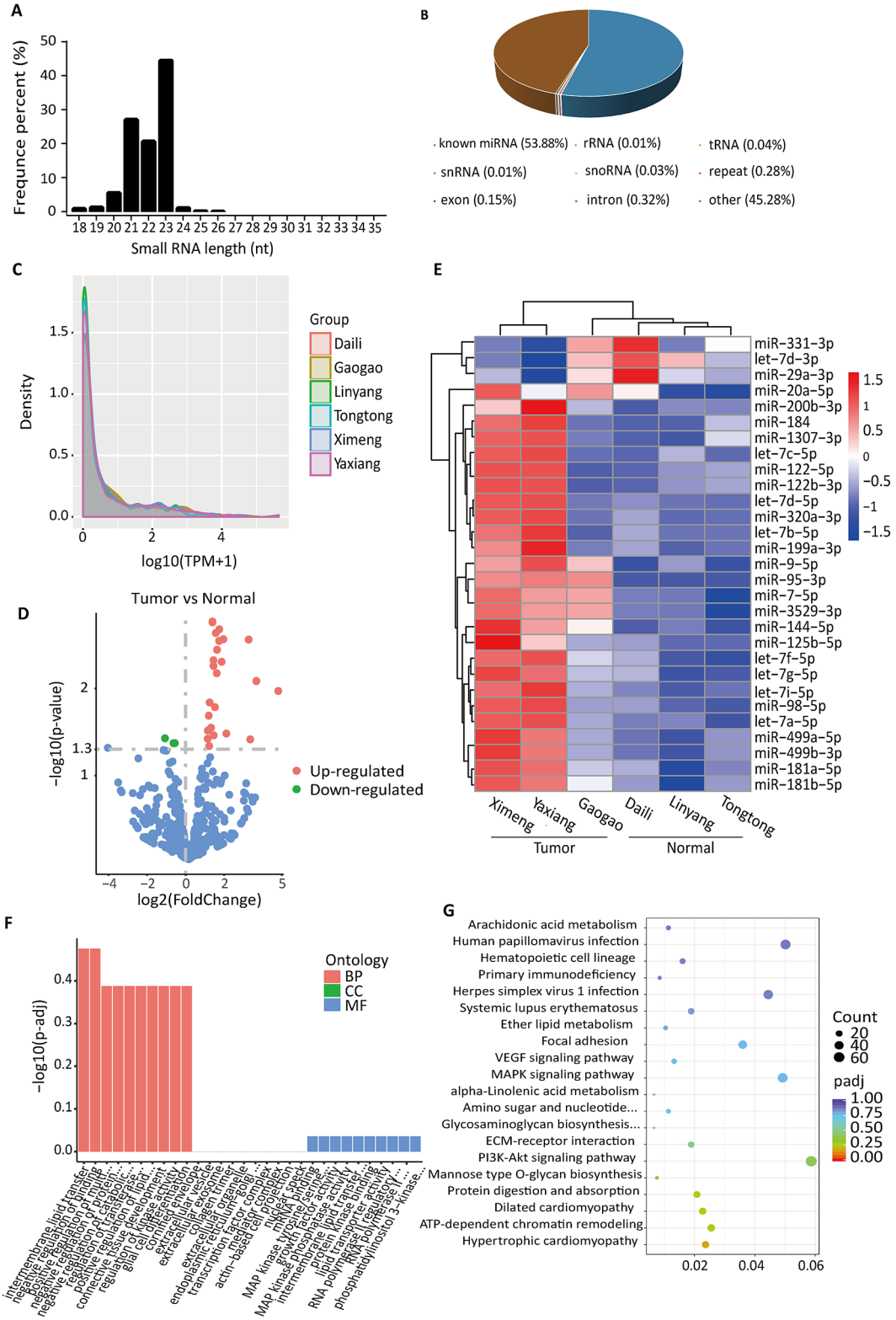

Fig. 2 Differential expression and functional enrichment of blood miRNAs in giant panda testicular tumor. **A** Length distribution with 18-35nt of all small RNA. **B** Category composition of all small RNA. **C** TPM density of miRNA expression. The miRNA expression level was represented by normalized log10 (TPM + 1) values. **D** Differentially expressed miRNAs statistics of giant pandas in tumor group and normal group. **E** Hierarchical cluster analysis of all differentially expressed miRNAs in tumor group and normal group. **F** GO enrichment analysis of target gene candidates. **G** Pathway assignment based on KEGG for target gene candidates of giant pandas

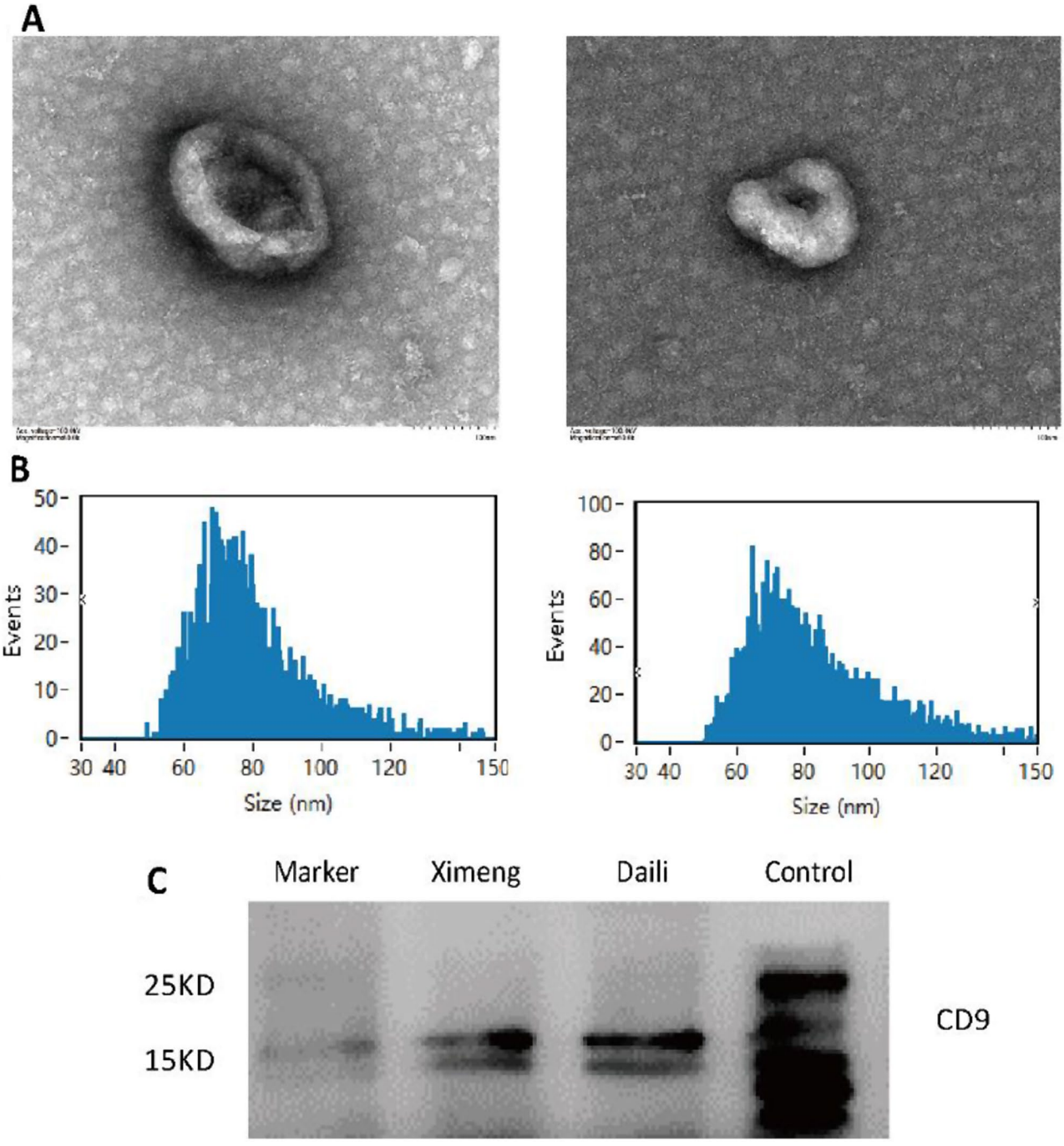

Fig. 3 Identification of exosomes. **A** Exosomes isolated from Ximeng and Daili were observed by TEM respectively. Acc. Voltage = 100.0Kv, Magnification = x60.0k, Scale bar, 100 nm. **B** Size distribution of exosomes isolated from Ximeng and Daili was analyzed using the particle size analyzer (NanoFCM, N30E) respectively. **C** Western blot of CD9 from exosomes, and the relative expression of CD9 was positive in Ximeng and Daili

dephosphorylation in biological processes, and extracellular matrix structural constituent, gated channel activity and ion gated channel activity in molecular function (Fig. 5D). KEGG analysis showed the relevant signaling pathways were mainly concentrated in Protein digestion and absorption, Leukocyte transendothelial migration and Nicotine addiction (Fig. 5E).

Correlation analysis of miRNA-mRNA expression and RT-PCR Validation

To determine the specific marker of testicular tumor of giant panda, spearman correlation analysis was conducted on miRNA-mRNA expression, and the results showed that only the expressions of miR-331-3p and *ENSAMEG00000004030* (*PKIG*) were

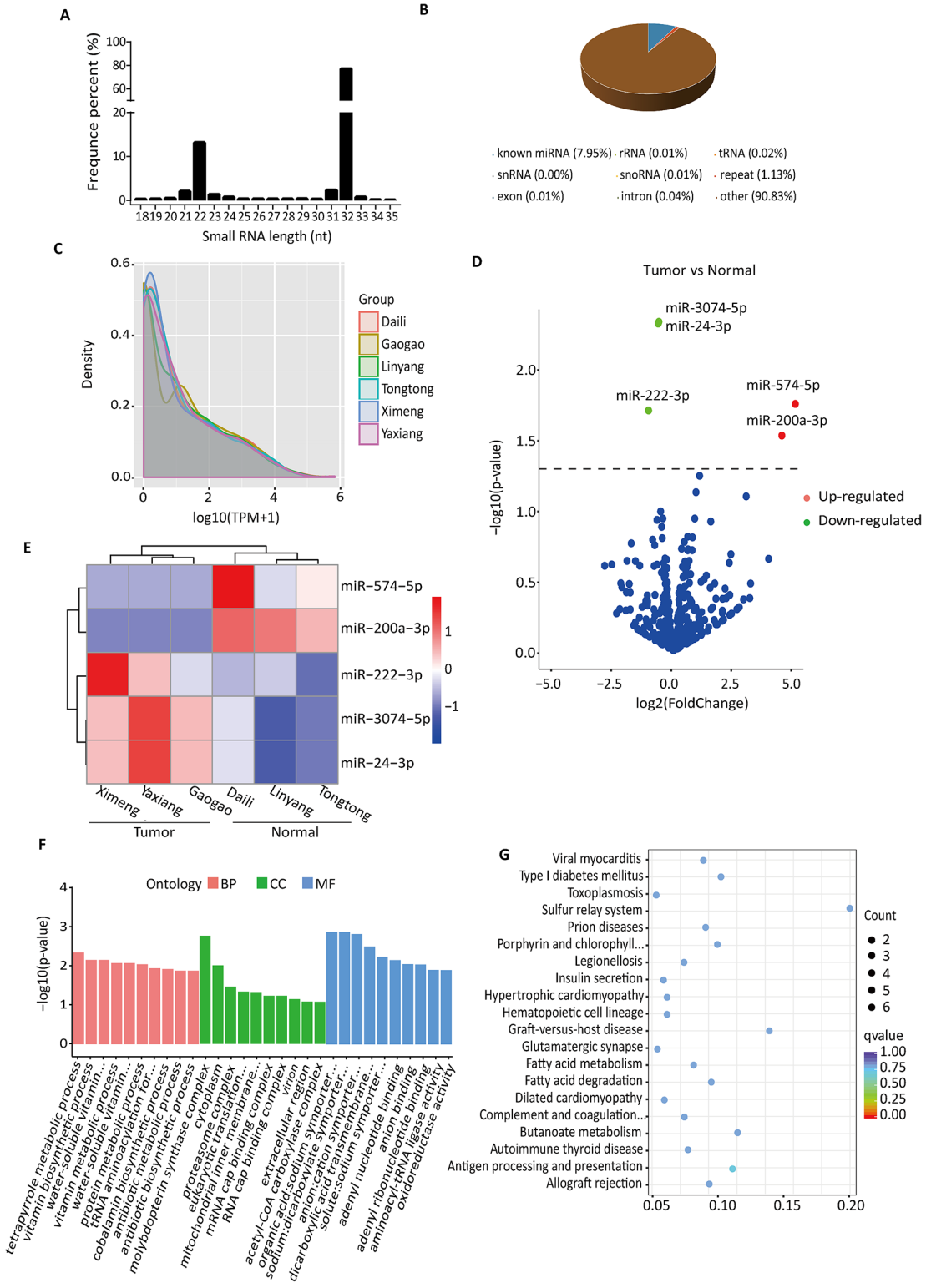

Fig. 4 Differential expression and functional enrichment of exosomal miRNAs. **A** Length distribution with 18-35nt of all small RNA. **B** Category composition of all small RNA. **C** TPM density of miRNA expression. **D** Differentially expressed miRNAs statistics of giant pandas in tumor group and normal group. **E** Hierarchical cluster analysis of all differentially expressed miRNAs in tumor group and normal group. **F** GO enrichment analysis of target gene candidates. **G** Pathway assignment based on KEGG for target gene candidates of giant panda

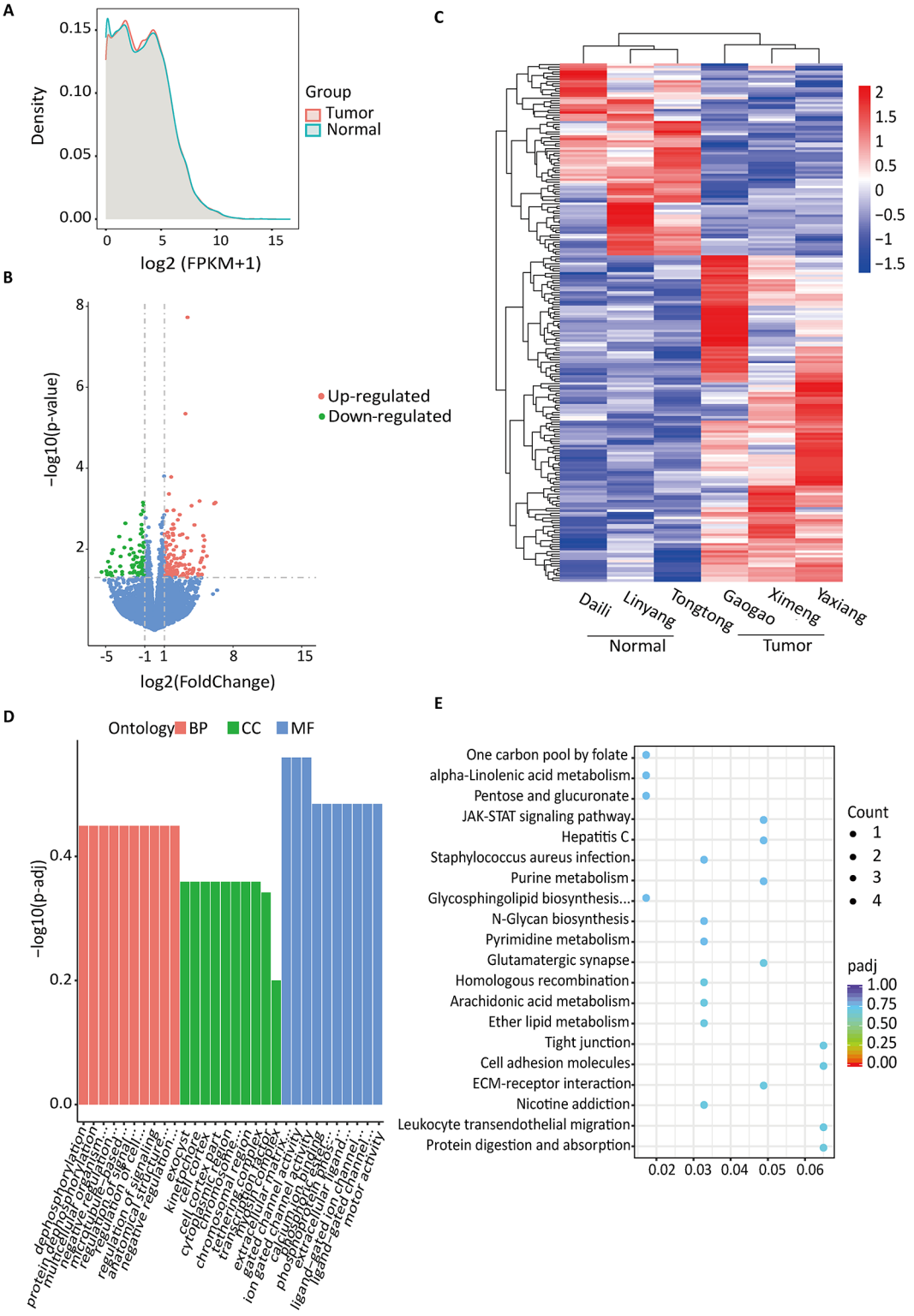

Fig. 5 Differential expression and functional enrichment of DEGs. **A** FPKM density of genes expression. **B** Differentially expressed genes statistics of giant pandas between tumor group and normal group with corrected p-value < 0.05 and |log2FoldChange| >1. **C** Hierarchical clustering heatmap of all differentially expressed genes between tumor group and normal group, and the red-blue spectrum represents the normalized FPKM values. **D-E** GO and KEGG enrichment analysis of DEGs with corrected p-value < 0.05

significantly positively correlated (spearman = 0.943, $p < 0.01$), while the expressions of miR-331-3p and *ENSAMEG00000013628* were significantly negatively correlated (spearman= -0.829, $p < 0.05$) (Fig. 6A)

Then, to further verify the above results, the expression of miR-331-3p, *PKIG* and *ENSAMEG00000013628* was quantified by RT-PCR, and primer information is shown in Table 3. Our results showed that compared to normal panda, the relative expression of miR-331-3p in tumor panda was significantly reduced ($p < 0.01$), which was consistent with the result of miRNA sequencing (Fig. 6B). However, the relative expression of *PKIG* and *ENSAMEG00000013628* were inconsistent with our sequencing results (Fig. 6C and D), we speculated that there may be individual differences between giant pandas or differences in detection sensitivity. Finally, we fully believed that miR-331-3p could be used as a potential diagnostic marker for giant panda testicular tumor

Discussion

Exosomes are formed by the invagination of intracellular lysosomal particles, including transmembrane proteins (such as CD9, CD63, CD37 and CD81), fusion proteins (such as GTPases), polyvesicular endosomal producing proteins (such as Alix and TSG101), lipids (such as cholesterol), sugars and nucleic acids, etc. These inclusions are important biological characteristics of exosomes and important mediators involved in intercellular communication and biological processes [23, 24]. The morphology was observed by transmission electron microscopy (TEM), and appeared as round or cup-shaped vesicles wrapped in lipid bilayer. Particle diameters can be measured using a particle size analyzer, with diameters ranging from 30 to 150 nm. Protein detection mainly uses Western blot or nano-flow qNano to detect the marker proteins contained in exosomes [25]. Currently, the commonly used marker proteins include CD9, CD63, CD81, TSG101, etc [26–29]. After plasma exosomes were extracted in this experiment, their morphology was observed under TEM, showing round or cup-shaped vesicles with a measured diameter ranging from 30–150 nm, and their surface marker protein CD9 was positive. After the above identification, the vesicle-like particles in plasma extracted in this experiment were consistent with the characteristics of exosomes [30] and confirmed as exosomes

Studies have found miRNAs in exosomes can be used as biomarkers to reflect the pathological changes of exosome-released tissues [31]. However, this study found differences between blood miRNAs and exosomal miRNAs. Blood smallRNA showed unimodal distribution in the length distribution range of 18-35nt, while exosomal smallRNA enriched with kit showed bimodal distribution, which was consistent with previous research results [22]. In the analysis of miRNAs differential expression, we found that 29 miRNAs were differentially expressed in blood, while only 5 miRNAs were differentially expressed in exosomes, which was consistent with Xie's research. Xie [32] found that compared with plasma-derived exosomes, miRNAs in plasma were differentially regulated in disease animal models. Differential changes in miRNAs can be detected in exosomes and plasma samples, suggesting that different mechanisms are activated when regulating exosomes or other carriers of miRNAs. At the same time, higher variability was also present in plasma samples compared to exosomes, and this high variability may be due to the complexity of miRNAs origin in plasma samples [32]

Functional enrichment analysis of target genes of blood DEmiRNAs showed that these target gene candidates were mainly involved in intermembrane lipid transfer. Membrane lipids are the main components of the cell membrane and separate the interior of the cell from the external environment by forming lipid bilayer [33, 34]. Membrane lipids play an important role in maintaining the structural integrity and fluidity of cell membranes, as well as cell signaling and communication [33]. Studies have shown that tumor cell metastasis goes through different stages and requires lipid-related structural adaptations, including changes in lipid membrane composition to invade other sites and overcome cell death mechanisms [35]. Phosphatidylinositol (PI) and other membrane lipids can be phosphorylated by enzymes to produce lipid second messengers, which play an important role in cell signaling pathway. In addition, lipids also alter metabolic crosstalk between the tumor microenvironment and its surrounding cells, for example, tumor cells can absorb lipids released by stromal cells, which in turn affect immune cell function [36]. KEGG pathway mainly focuses on ATP-dependent chromatin remodeling and protein digestion and absorption. ATP-dependent chromatin remodeling complex plays an important role in development [37]. Genomic aberrations in genes encoding chromatin remodeling components can lead to different malignancies, such as pancreatic ductal adenocarcinoma (PDAC) [38–40]. In pancreatic cancer, chromosome aberrations and/or mutations associated with ATP-dependent chromatin remodeling complexes were detected in approximately 1/3 of the samples [41, 42], highlighting the role of abnormal chromatin remodeling in tumorigenesis

Functional enrichment analysis of target genes of exosomal DEmiRNAs showed that the relevant signaling pathways were mainly concentrated in antigen processing and presentation. The processing and presentation of neoantigens play a key role in the immunotherapy of lung cancer. Immunotherapy uses the patient's own immune function to recognize and kill tumor cells by activating

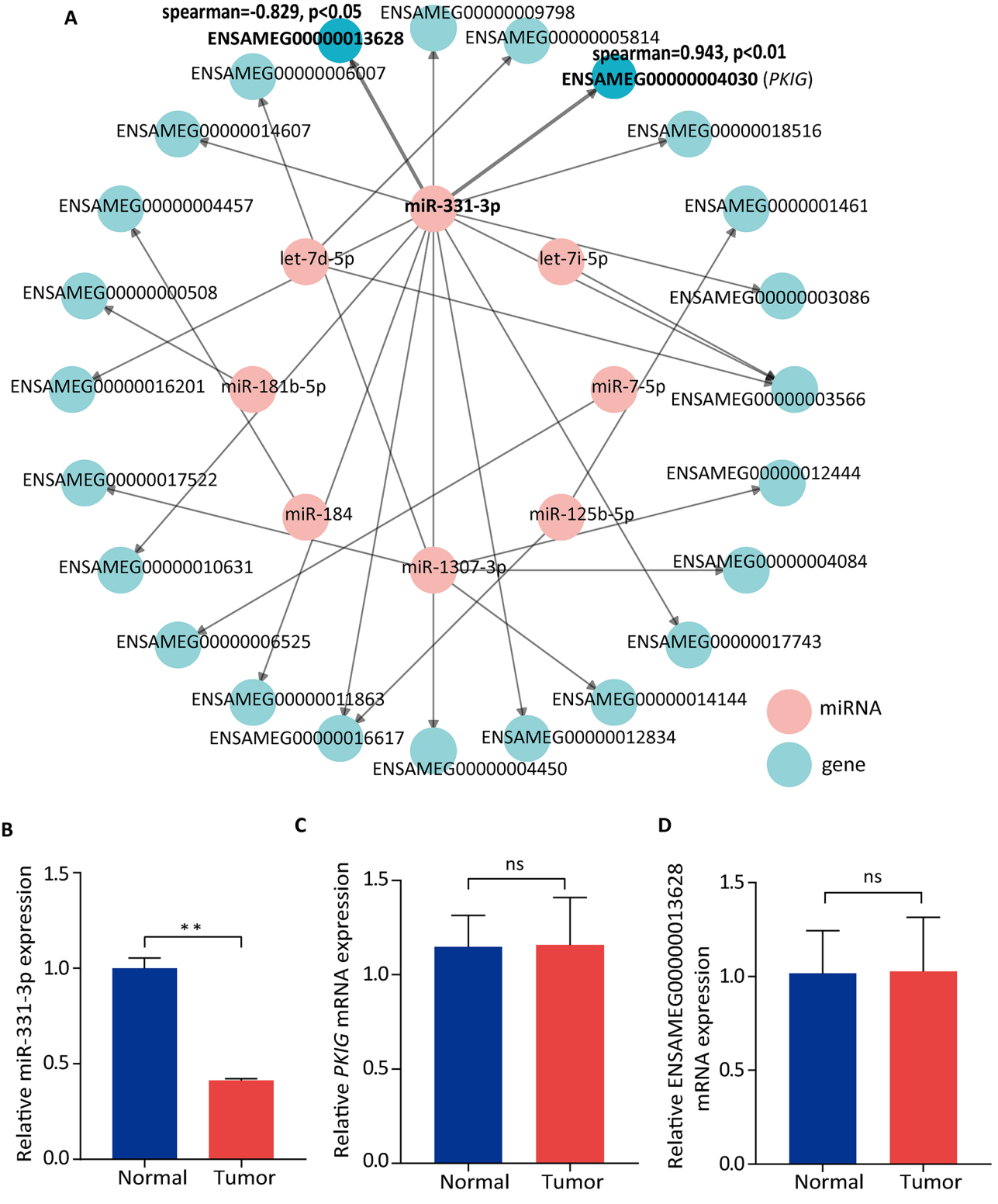

Fig. 6 Correlation analysis of miRNA-mRNA expression and RT-PCR. **A** Spearman correlation regulatory network analysis of a part of miRNA-mRNA expression. **B** The relative expression of miR-331-3p in normal and tumor giant pandas, *U6* was used as reference gene. **C** The relative mRNA expression of *PKIG* in normal and tumor giant pandas, *GAPDH* was used as reference gene. **D** The relative mRNA expression of *ENSAMEG00000013628* in normal and tumor giant pandas. These data are expressed as mean ± S.D. of three independent experiments. ns = not significant. * $p < 0.05$, ** $p < 0.01$ compared with control

Table 3 Primer information for RT-PCR

Name	Primer sequence
miR-331-3p	F-TCGCCCCTGGGCCTATC
	R-ACTGCAGGGTCCGAGGTATT
PKIG	F-TCCTCCTACTCGGACTTCATTTC
	R-ACCTCTGTCTGCCCTTCTGC
ENSAMEG00000013628	F-CACGCTCTTCTTGCCATTCTC
	R-TTGGAGGGCTTGGTGGTCT
U6	F-CTCGCTTCGGCAGCACA
	R-AACGCTTCACGAATTTGCGT
GAPDH	F-TCAAGAAGGTGGTGAAGCAGG
	R-CGGCATCAAAGGTGGAAGAGT

the activity of $CD8^+$ T cells. Therefore, effective antigen presentation is essential for $CD8^+$ T cell-mediated immune responses [43, 44]. Previous studies have shown that tumor cells can achieve immune escape by reducing antigen presentation through the regulation of antigen processing and presentation pathways [45]. Therefore, we speculate that the pathogenic mechanism of giant panda testicular tumor may be related to the regulation of antigen processing and presentation pathway and then affect related immune function, but further study is still needed

GO analysis showed that tumor-specific DEGs significantly enriched dephosphorylation and protein dephosphorylation. Protein phosphorylation is the most basic and important mechanism to regulate and control protein activity and function, and protein tyrosine phosphorylation is essential for the proper function of cells and organisms [46]. Alterations in phosphorylation pathways can lead to serious diseases, especially cancer. Many signaling pathways including tyrosine kinases and cyclin-dependent kinases, calmucin-catenin complexes are major players in the cell cycle, and dysregulation in their phosphorylation response has been shown in various types of cancer. Tyrosine phosphorylation is accomplished by protein tyrosine kinases (PTKs), the family of tyrosine kinases that covers the most oncogene proteins [47]. Studies have shown that MAPK plays an important role in cancer growth and progression, Bcl-2 family proteins have pro-apoptotic or anti-apoptotic functions, and cyclin is a key regulator of the cell cycle. Phosphorylation changes in any of these pathways are closely associated with cancer, and they also serve as potential products for anticancer drug development [48]. Therefore, we speculate that pathogenesis of giant panda testicular tumor may be related to protein phosphorylation of a certain pathway, which needs further investigation.

miR-331-3p is closely related to the development of cancer. Studies have found that miR-331-3p may be involved in the regulation of cell growth and cell cycle, so it may initially be considered as a tumor suppressor [49]. In recent years, the role of miR-331-3p in tumors has attracted increasing attention, and the expression of miR-331-3p has been significantly down-regulated in gastric cancer [50], prostate cancer [51]and glioblastoma [52]. In colorectal cancer cells, overexpression of miR-331-3p inhibits cell growth, promotes cell apoptosis and activates cysteine aspartic protease 3 (Caspase-3) by inhibiting the expression of human epidermal growth factor receptor 2 (HER2) [53]. In gastric cancer, miR-331-3p, as a key regulator of cell proliferation, leads to cell cycle arrest by directly inhibiting *E2F1* gene expression [50]. Therefore, miR-331-3p can be considered as a tumor suppressor gene. On the other hand, miR-331-3p plays a carcinogenic role in hepatocytes by directly targeting PH domains and leucine-rich repeat protein phosphatases, thereby promoting cell proliferation and metastasis [54]. Our study showed that the expression of miR-331-3p was also significantly reduced in of giant panda testicular tumor. Meanwhile, the combined analysis of miRNA-mRNA showed that miR-331-3p was significantly positively correlated with *PKIG* expression. We hypothesized that miR-331-3p may be involved in the regulation of the occurrence and development of in giant panda testicular tumor through coordination with *PKIG*. cAMP-dependent protein kinase inhibitor gamma (*PKIG*), also known as *PKI-gamma*, is widely expressed in various tissues such as heart, bladder and testis, and is an effective competitive camp-dependent protein kinase inhibitor. Studies have shown that the protein encoded by *PKIG* is involved in osteoblast and adipocyte differentiation [55]. However, our RT-PCR results showed that the expression of *PKIG* was inconsistent with that of sequencing, and we speculated that there might be two reasons, first, due to the rarity of giant panda samples, we conducted RT-PCR on fewer samples, and there might be individual differences; second, there are differences in the sensitivity of sequencing and RT-PCR. Therefore, miR-331-3p is only a preliminary reference for judging giant panda testicular tumor, and we will make a comprehensive judgment based on phenotypic characteristics and pathological analysis. In the future, we will continue to collect clinical data and continue to verify the role of miR-331-3p as a potential diagnostic marker for giant panda testicular tumors.

Conclusions

Through miRNA-mRNA sequencing, we found blood miRNAs and exosomal miRNAs have different regulatory patterns, which may reflect different biological processes in the pathogenesis of testicular tumor. Meanwhile, miR-331-3p could be used as a potential diagnostic marker for giant panda testicular tumor. Our findings are conducive to the rapid clinical diagnosis of giant panda testicular tumor, and are also expected to provide scientific reference for further research on the pathogenesis of testicular tumor.

Supplementary Information

The online version contains supplementary material available at https://doi.org/10.1186/s12917-024-04326-y.

Supplementary Material 1

Supplementary Material 2

Acknowledgements
Not applicable.

Author contributions
D.S.L, Z.H., C.D.W. and Y.Z. devised the experiment. M.W., K.W. and L.H.D. collected blood samples. B.Y. and X.M.C. performed the experiments. W.W.D., Q.Y.Y. and X.Z. analyzed the data. C.W.L. and Y.Z. prepared the figures and tables. C.Y.L. and Y.Z. prepared the manuscript. Q.L. coordinated funds. All authors read and approved the final manuscript.

Funding
This research was supported by Key Technologies of Wild Giant Panda Population and Habitat Protection in Giant Panda National Park (No. CGF2024001) and China Conservation and Research Center for the Giant Panda Fund Project (No. CCRCGP222316).

Data availability
The datasets generated and/or analysed during the current study are available in the Genome Sequence Archive (GSA), and the accession numbers were CRA018282, CRA018284 and CRA018288.

Declarations

Ethics approval and consent to participate
The animal study was approved by The Conservation and Research Center for the Giant Panda Ethical Review Committee for Experimental Animals, Conservation and Research Center for the Giant Panda. The study was conducted in accordance with the local legislation and institutional requirements.

Consent for publication
Not applicable.

Competing interests
The authors declare no competing interests.

Author details
[1]State Forestry and Grassland Administration Key Laboratory of Conservation Biology for Rare Animals of the Giant Panda State Park, China Conservation and Research Center for the Giant Panda, Chengdu 610081, China

Received: 8 August 2024 / Accepted: 10 October 2024
Published online: 15 November 2024

References

1. Gilligan T, Lin D, Aggarwal R, Chism D, Pluchino L. Testicular Cancer, Version 2.2020, NCCN Clinical Practice guidelines in Oncology. J Natl Compr Canc Netw. 2019;17(12):1529–54.
2. Wei W, Yi X. Progress in early diagnosis and treatment of malignant testicular tumors. J Contemp Urol Reprod Oncol. 2023;15(2):121–4.
3. Ulbright TM. The most common, clinically significant misdiagnoses in Testicular Tumor Pathology, and how to avoid them. Adv Anat Pathol. 2008;15(1):18–27.
4. Liu B. Testicular tumors of domestic animals. GUANGDONG J Aimal Veterinary Sci. 1994;19(4):21–4.
5. Liu H, Li R, Liu T, Yang L, Xie Q. Immunomodulatory effects of mesenchymal stem cells and mesenchymal stem cell-derived extracellular vesicles in rheumatoid arthritis. Front Immunol. 2020;11:1912.
6. Zhou Z, Tang X. Research progress on the role of exosomal miRNA in the occurrence and development of tumors. Chin Bull Life Sci. 2019;31(6):551–7.
7. Ahmadi M, Jafari R, Mahmoodi M, Rezaie J. The tumorigenic and therapeutic functions of exosomes in Colorectal Cancer: opportunity and challenges. Cell Biochem Funct. 2021;39(4):468–77.
8. Sohn W, Kim J, Kang SH, Yang SR, Paik YH. Serum exosomal microRNAs as novel biomarkers for hepatocellular carcinoma. Exp Mol Med. 2015;47(9):e184.
9. Lai X, Wang M, Mcelyea SD, Sherman S, House M, Korc M. A microRNA signature in circulating exosomes is superior to exosomal glypican-1 levels for diagnosing pancreatic cancer. Cancer Lett. 2017;393:86–93.
10. Li XJ, Ren ZJ, Tang JH, Yu Q. Exosomal MicroRNA MiR-1246 promotes Cell Proliferation, Invasion and Drug Resistance by Targeting CCNG2 in breast Cancer. Cell Physiol Biochem. 2017;44(3):1741–8.
11. Meng X, Volkmar M, Karin ML, Fabian T, Klaus P, Heidi S. Diagnostic and prognostic relevance of circulating exosomal miR-373, miR-200a, miR-200b and miR-200c in patients with epithelial ovarian cancer. Oncotarget. 2016;7(13):16923–35.
12. Mihelich B, Dambal S, Lin S, Nonn L. miR-182, of the miR-183 cluster family, is packaged in exosomes and is detected in human exosomes from serum, breast cells and prostate cells. Oncol Lett. 2016;12(2):1197–203.
13. Shi R, Wang PY, Li XY, Chen JX, Li Y, Zhang XZ, Zhang CG, Jiang T, Li WB, Ding W. Exosomal levels of miRNA-21 from cerebrospinal fluids associated with poor prognosis and tumor recurrence of glioma patients. Oncotarget. 2015;6(29):26971–81.
14. Zhou L, Chen J, Li Z, Li X, Hu X, Huang Y. Integrated Profiling of MicroRNAs and mRNAs: MicroRNAs located on Xq27.3 associate with Clear Cell Renal Cell Carcinoma. PLoS ONE. 2010;5(12):e15224.
15. Love MI, Huber W, Anders S. Moderated estimation of Fold change and dispersion for RNA-seq data with DESeq2. Genome Biol. 2014;15(12):550.
16. Storey JD. The positive false discovery rate: a bayesian interpretation and the q -. Ann Stat. 2003;31(6):2013–35.
17. Enright AJ, John B, Gaul U, Tuschl T, Sander C, Marks DS. MicroRNA targets in Drosophila. Genome Biol. 2003;5:R1.
18. John B, Enright AJ, Aravin A, Tuschl T, Sander C, DS M. Human MicroRNA targets. PLoS Biol. 2005;3(7):e264.
19. Langmead B, Trapnell C, Pop M, Salzberg SL. Ultrafast and memory-efficient alignment of short DNA sequences to the human genome. Genome Biol. 2009;10:R25.
20. Mao XZ, Cai T, Olyarchuk JG, Wei LP. Automated genome annotation and pathway identification using the KEGG Orthology (KO) as a controlled vocabulary. Bioinformatics. 2005;21(19):3787–93.
21. Yu G, Wang LG, Han Y, He QY. clusterProfiler: an R package for comparing biological themes among gene clusters. OMICS. 2012;16(5):284–7.
22. Jiang L, Schlesinger F, Davis C, Zhang Y, Li R, Salit M, Gingeras T, Oliver B. Synthetic spike-in standards for RNA-seq experiments. Genome Res. 2011;21(9):1543–51.
23. Nabariya DK, Pothuraju R, Reddanna P, Yenuganti VR. Exosomes: the protagonists in the tale of colorectal cancer. Biochim Biophys Acta Rev Cancer. 2020;1874(2):188426.
24. Bao YJ, Zhu LY. Research progress in exosomal miRNA as tumor microenvironment regulators. Clin Med Res Pract. 2022;7(11):192–5.
25. Shao H, Hyungsoon I, Castro C, Weissleder B. New Technologies for Analysis of Extracellular Vesicles. Chem Rev. 2018;118(4):1917–50.
26. Pang Y, Liang S, Wen C, Chen M, Lu C, Wei K, Pan Y, Liang X. Isolation and identification of plasma exosomes in Buffalo Calve. China Anim Husb Veterinary Med. 2021;48(9):3200–5.
27. Caby M, Lankar D, laude V, Raposo G, Bonnerot C. Exosomal-like vesicles are present in human blood plasma. Int Immunol. 2005;17(7):879–87.
28. Kim J, Tan Z, ML D. Exosome enrichment of human serum using multiple cycles of centrifugation. Electrophoresis. 2015;36:2017–26.
29. Vlassov AV, Magdaleno S, Setterquist R, Conrad R. Exosomes: current knowledge of their composition, biological functions, and diagnostic and therapeutic potentials. Biochim Biophys Acta. 2012;1820(7):940–8.
30. Lara S, Lavaniya T, Nickolai V, Sinden JD, Costanza E. Investigation of content, stoichiometry and transfer of miRNA from human neural stem cell line derived exosomes. PLoS ONE. 2016;11(1):e0146353.
31. Liu N, Zhang G, Yao Q. Research progress of exosomal mirnas and their use as tumor molecular markers. Lab Med Clin. 2021;18(3):417–20.
32. Xie J, Fan X, Christopher A, Reetam M, Xie Y, Chen T. MicroRNA profiling in kidney disease: plasma versus plasma-derived exosomes. Gene. 2017;627:1–8.

33. Bruno S, Julia S, Kaspar PL. Membrane lipids and transporter function. Biochim et Biophys acta Mol Basis Disease: BBA. 2021;1867(5):1–11.
34. Meer GV, Voelker DR, Feigenson GW. Membrane lipids, where they are and how they behave. Nat Rev Mol Cell Biol. 2008;9(2):112–24.
35. Miguel M, Uxue U, Claudia B, Salvador A. The role of lipids in cancer progression and metastasis. Cell Metabol. 2022;34(11):1675–99.
36. Broadfield LA, Pane AA, Talebi A, Swinnen JV, Fendt SM. Lipid metabolism in cancer: new perspectives and emerging mechanisms. Dev Cell. 2021a;56:1363–93.
37. Hasan N, Ahuja N. The emerging roles of ATP-Dependent chromatin remodeling complexes in pancreatic Cancer. Cancers. 2019;11(12):1859–95.
38. Gwen L, Yuna B, Rémy N, Asha N, Krutika S, Laetitia M. Distinct epigenetic landscapes underlie the pathobiology of pancreatic cancer subtypes. Nat Commun 2018, 9(1978).
39. Bracken AP, Brien GL, Verrijzer CP. Dangerous liaisons: interplay between SWI/SNF, NuRD, and Polycomb in chromatin regulation and cancer. Genes Dev. 2019;33:936–59.
40. Ho L, Crabtree GR. Chromatin remodelling during development. Nature. 2010;463(7280):474–84.
41. Witkiewicz AK, Mcmillan EA, Balaji U, Baek GH, Lin WC, Mansour J, Mollaee M, Wagner KU, Koduru P, Yopp A. Whole-exome sequencing of pancreatic cancer defines genetic diversity and therapeutic targets. Nat Commun. 2015;6:6744.
42. Shain AH, Giacomini CP, Matsukuma K, Karikari CA, Bashyam MD, Hidalgo M, Maitra A, Pollack JR. Convergent structural alterations define SWItch/Sucrose NonFermentable (SWI/SNF) chromatin remodeler as a central tumor suppressive complex in pancreatic cancer. Proc Natl Acad Sci USA. 2012;109(5):1370–1.
43. Alexander C, Huang MA, Postow RJ, Orlowski RM, Bertram B, Manne S. T-cell invigoration to tumour burden ratio associated with anti-PD-1 response. Nature. 2017;545(7652):60–5.
44. Han JF, Chen K, Wang C, Chen F, Li W. Acquired Resistance to Anti-PD-1 Therapy Induced by Mutant PSMB5 Down-Regulation Antigen Processing and Presentation in Non-Small cell Lung Cancer. J Evidence-Based Med. 2023;23(1):47–53.
45. Suchit J, Christian H. Antigen presentation in cancer: insights into tumour immunogenicity and immune evasion. Nat Rev Cancer. 2021;21(5):298–312.
46. Hunter T. Signaling–2000 and beyond. Cell. 2000;100(1):113–27.
47. Elson A. Stepping out of the shadows: oncogenic and tumor-promoting protein tyrosine phosphatases. Int J Biochem Cell Biology. 2018;96:135–147.
48. Singh V, Ram M, Kumar R, Prasad R, Roy BK, Singh KK. Phosphorylation: implications in Cancer. Protein J. 2017;36(1):1–6.
49. Maes OC, Sarojini H, Wang E. Stepwise up-regulation of MicroRNA expression levels from replicating to reversible and irreversible growth arrest states in WI-38 human fibroblasts. J Cell Physiol. 2009;221(1):109–19.
50. Guo X, Guo L, Ji J. miRNA-331-3p directly targets E2F1 and induces growth arrest in human gastric cancer. Biochem Biophys Res Commun. 2010;398(1):1–6.
51. Epis MR, Barker A, Giles KM, Beveridge DJ, Leedman PJ. The RNA-binding protein HuR opposes the repression of ERBB-2 gene expression by microRNA mir-331-3p in prostate cancer cells. J Biol Chem. 2011;286(48):41442–54.
52. Epis MR, Giles KM, Candy PA, Webster RJ, Leedman PJ. Mir-331-3p regulates expression of neuropilin-2 in glioblastoma. Neurooncol 2014, 116(1):67–75.
53. Zhao D, Sui Y, Zheng X. Mir-331-3p inhibits proliferation and promotes apoptosis by targeting HER2 through the PI3K/Akt and ERK1/2 pathways in colorectal cancer. Oncol Rep. 2016;35(2):1075–82.
54. Chang R, Yang H, Fang F, Xu J, Yang L. MicroRNA-331-3p promotes proliferation and metastasis of hepatocellular carcinoma by targeting PH domain and leucine-rich repeat protein phosphatase. Hepatology. 2014;60(4):1251–63.
55. Chen X, Hausman BS, Luo G, Zhou G, Murakami S, Rubin J, Greenfield EM. Protein kinase inhibitor γ reciprocally regulates osteoblast and adipocyte differentiation by downregulating leukemia inhibitory factor. Stem Cells. 2013;31:2789–99.

Publisher's note